Late Holocene palaeoceanography in Van Mijenfjorden, Svalbard

Morten Hald, Torbjörn Dahlgren, Tor-Eirik Olsen & Erland Lebesbye

Based on detailed stratigraphical analysis of sediment cores spanning the last ca. 4000 calendar years, we reconstruct the palaeoceanograhic changes in the fiord Van Mijenfjorden, western Svalbard. Benthic foraminiferal $\delta^{18}O$ indicate a gradual reduction in bottom water salinities between 2200 BC and 500 BC. This reduction was probably mainly a function of reduced inflow of oceanic water to the fiord, due to isostatic shallowing of the outer fiord sill. Stable salinity conditions prevailed between 500 BC and. 1300 AD. After the onset of a major glacial surge of the tidewater Paulabreen (Paula Glacier) system (PGS) around 1300 AD, there was a foraminiferal faunal change towards glacier proximal conditions, associated with a slight bottom water salinity depletion. During a series of glacial surges occuring from 1300 AD up the present salinity in the fiord has further decreased, corresponding to a $\delta^{18}O$ depletion of 0.5 ‰. This salinity decrease corresponds to the period when the PGS lost an equivalent of 30 - 40 % of its present ice volume, mainly through calving in the fiord.

M. Hald, T. Dahlgren, T.-E. Olsen & E. Lebesbye, Dept. of Geology, University of Tromsø, N-9037 Tromsø, Norway.

Studies of forcing factors for rapid climatic change in the past are important in order to better model future change. Arctic fiords represent areas where such studies should be undertaken for several reasons. 1) They include settings with high sediment input. From these we can obtain sediment cores of high resolution, enabling studies of past changes on centennial to decadal time scales. 2) They may provide recent and sub-recent analogues to Quaternary glaciomarine settings of shelves and fiords. 3) They may improve our understanding of climatic responses of ocean–glacier interactions in general, and in particular elucidate how surging glaciers may have climatic and oceanographic effects.

The Svalbard Archipelago, situated between 76° and 80° N, is bordered by the Arctic Ocean to the north, the Barents Sea to the south and east, and the Greenland Sea to the west (Fig. 1). Glaciers cover some 62 % of the archipelago and many glaciers reach the Svalbard fiords as tidewater glaciers. The purpose of this paper is to elucidate the oceanic response over time to tidewater glacier fluctuations in Van Mijenfjorden in western Svalbard. In particular we investigate the effect of the surge-type Paulabreen system from 1300 AD to the present.

Physiographic setting

Svalbard's fiords have a typical glacial morphology that includes troughs and sills. Van Mijenfjorden (Fig. 1), the second largest fiord in western Svalbard, is 50 km long and ca. 10 km broad. It has restricted oceanic communication due an extreme outer sill formed by the island Akseløya. The fiord is divided into three basins. Maximum

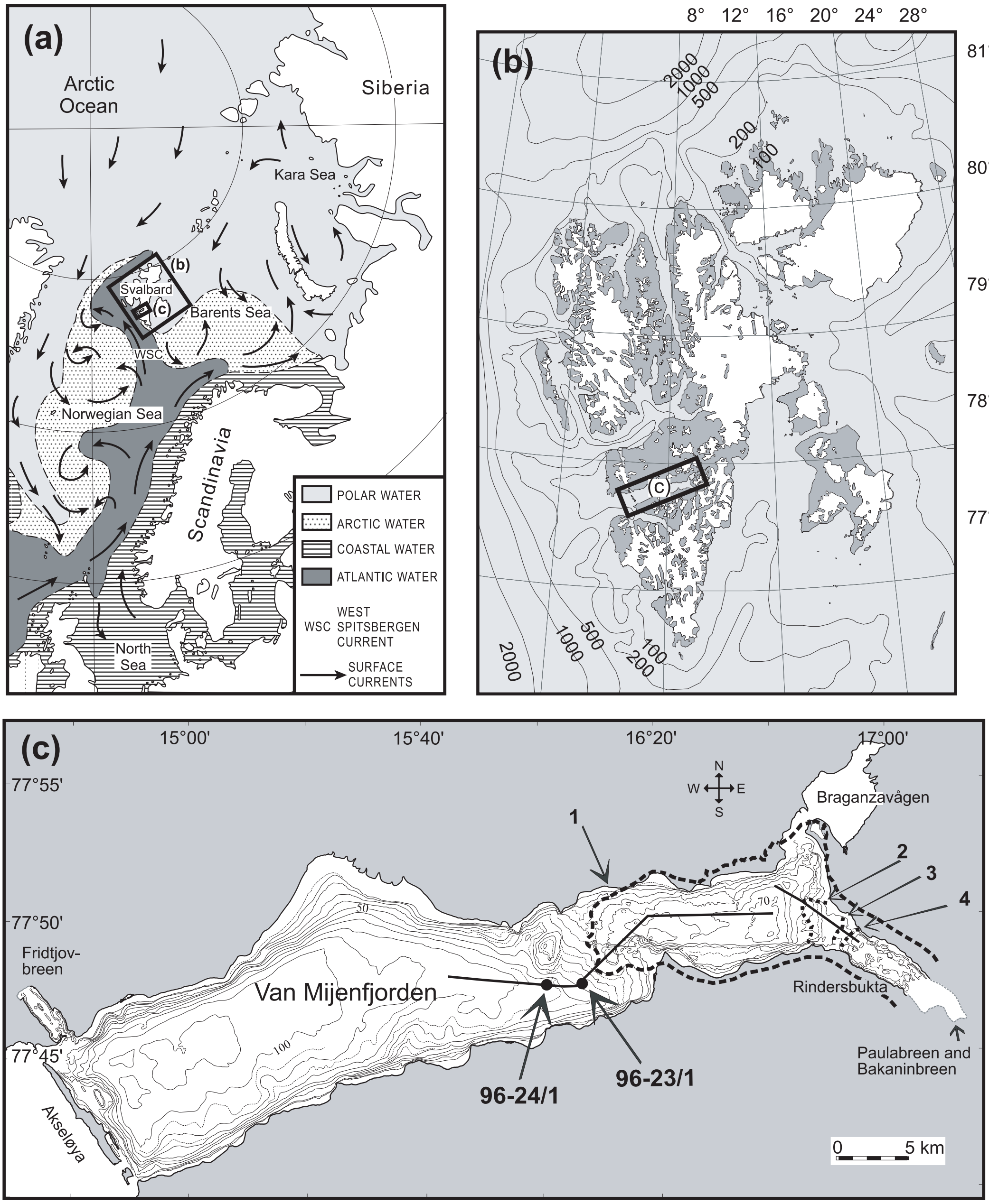

Fig. 1. Location map showing: (a) major surface water masses of the Norwegian–Greenland Sea and adjacent seas; (b) the Svalbard Archipelago; and (c) detailed bathymetric map of Van Mijenfjorden indicating location of the sediment cores (black dots), acoustic profiles (solid lines) and ice margin positions (broken lines) during the 1300 AD glacial surge (1) and three younger surge events (2, 3 & 4).

depth of the outer basin is 112 m as compared to 74 m in the middle basin and ca. 30 m in the inner basin (Rindersbukta). Most of the fiord is located within Paleogene sedimentary bedrock of various types such as sandstones, siltstones, shales, coals and coal pebbles (Steel & Worsley 1984). Early Cretaceous sedimentary rocks are found in the innermost part. Further inland shales of the Janus

Formation crop out (Salvigsen & Winsnes 1989). The overlying Cretaceous strata (Helvetiafjellet and Carolinefjellet formations) are mainly composed of alternating shales, sand- and siltstones, including coal and thin impure limestones. In the outer parts of the fiord there is a westward shift from early Cretaceous, Jurassic, Triassic, Carboniferous–Permian to Vendian (Proterozoic) bedrock (Harland 1997).

The catchment area of Van Mijenfjorden is approximately 2.8 x 103 km^2; 50 % of this area is covered by glaciers (Hagen et al. 1993). A tidewater glacier, Fridtjovbreen, is located in the northern outermost parts of Van Mijenfjorden. This glacier started to surge in 1997 and several glaciers in Svalbard are surge-type (Murray et al. 1998; Jiskoot et al. 2000). The fiord head is occupied by the large tidewater glacier system of Paulabreen (PGS), of which Paulabreen and Bakaninbreen (Bakanin Glacier) are the only remaining glaciers in Van Mijenfjorden today. Several tributary glaciers feed the main glaciers of the PGS. All the glaciers in the area have experienced a significant loss of volume during the last century (Hagen et al. 1993).

Oceanography

Svalbard is influenced by relatively warm Atlantic Water transported from the south via the West Spitsbergen Current, and by Polar Water and Arctic Water from the north (Fig. 1). The sea ice conditions around Svalbard vary according to the season, degree of exposure to storm waves, and response to the oceanic circulation around the archipelago (Dowdeswell & Dowdeswell 1989). A continuous cover of fast ice forms in the major fiord systems and in other sheltered coastal areas with restricted geometry by about late November and usually remains until late May or June (Wadhams 1981). Arctic pack ice is usually present around north-east Svalbard throughout the year, with the lowest flow densities in August and September (Vinje 1985). Between November and April the pack ice may surround the entire archipelago, with minimum densities on the west coast of Spitsbergen. The asymmetric distribution of polar pack ice results from oceanic circulation in which polar waters transport pack ice southward on the eastern side of Svalbard and the West Spitsbergen Current brings warm Atlantic Water northward to the western coast of Svalbard (Wadhams 1981; Vinje 1985) (Fig. 1).

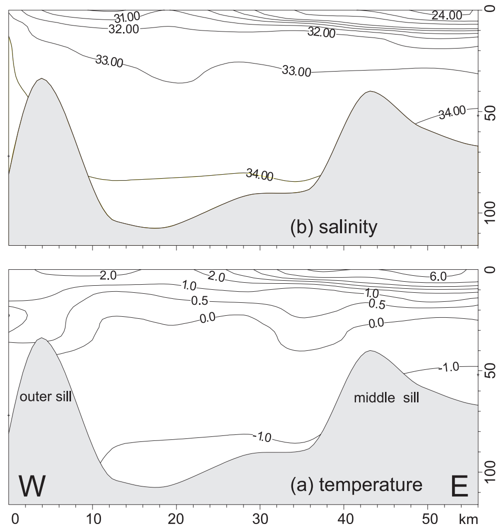

Fig. 2. Hydrographic transect in Van Mijenfjorden showing the distribution in the water column of (a) salinity (psu) and (b) temperature (°C). (Figure modified from Skardhamar 1998; printed with permission of the author.)

The mouth of Van Mijenfjorden is almost closed from the open ocean by the island Akseløya and thus allows only for a very modest inflow of Atlantic Water (Fig. 1). The sea-floor surface sediments are dominantly silty clay (Hald & Korsun 1997). The water column is dominated by cold Local Water, with bottom water temperatures of around –1 °C and a seasonally warmed surface layer (Fig. 2). Gulliksen et al. (1985) reported a minimum July bottom water temperature of -1.5 °C. Bottom water salinity is around 34 ‰ in the two outer basins and a pycnocline is observed in the upper 10 - 15 m.

Late Holocene glacial history of the Paulabreen system

The characteristic marine diamictons on land in the inner part of Van Mijenfjorden have provoked many investigators to address the glacial history of the area. These diamictons contain bivalve shells and show a typical hummocky morphology and little vegetation cover. As early as 1911 they were interpreted by Högbom (1911) as having been deposited by a rapid advance (surge) of the Paulabreen system (PGS). During the advance, the PGS picked up marine sediments and incor-

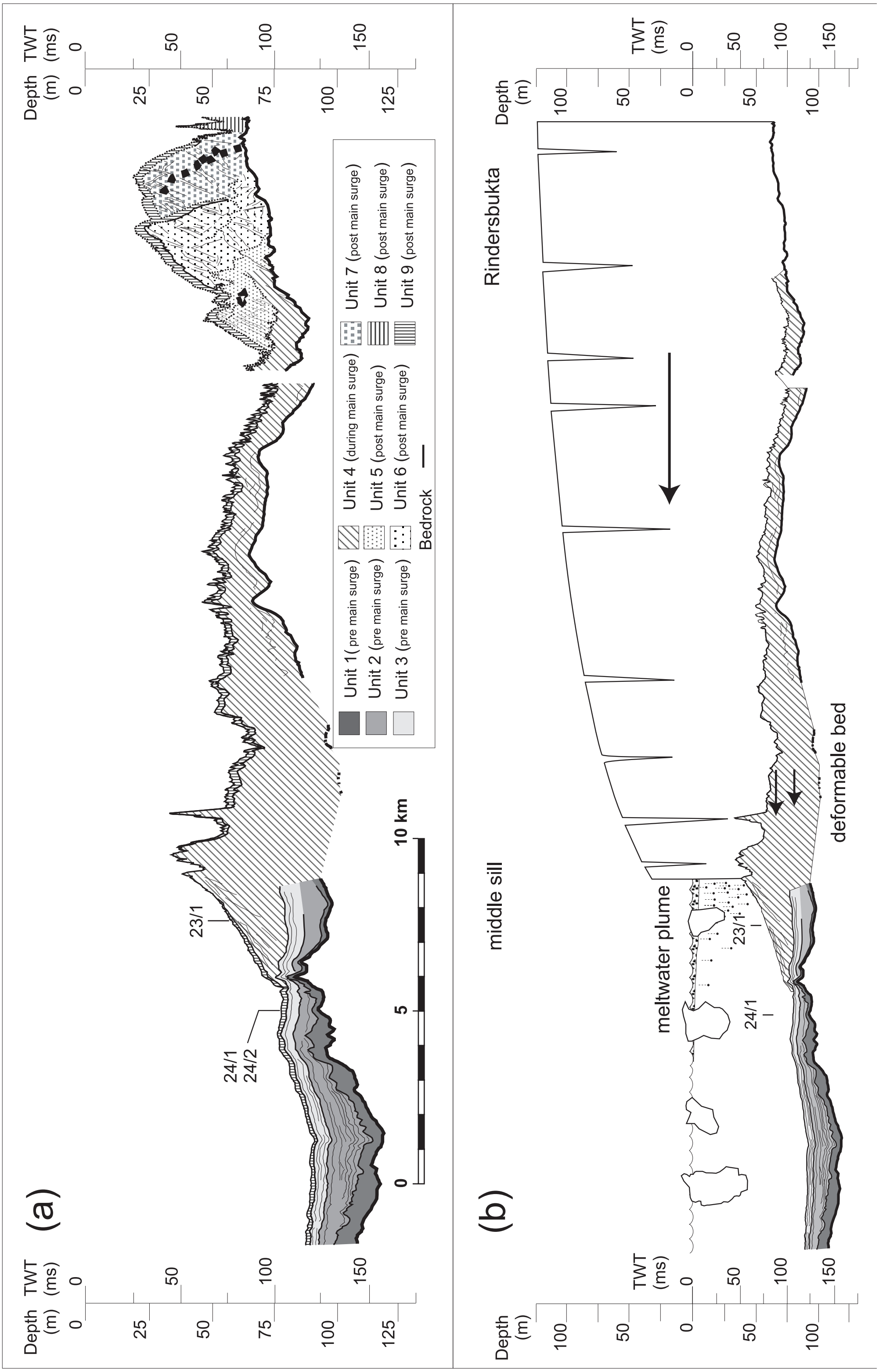
(a)
(b)
Depth (m)
TWT (ms)
0
25
50
75
100
125
150
0
5
10 km
24/1
24/2
23/1
Unit 1 (pre main surge)
Unit 2 (pre main surge)
Unit 3 (pre main surge)
Unit 4 (during main surge)
Unit 5 (post main surge)
Unit 6 (post main surge)
Unit 7 (post main surge)
Unit 8 (post main surge)
Unit 9 (post main surge)
Bedrock
meltwater plume
middle sill
Rindersbukta
deformable bed

porated them into the diamicton of the moraines (Högbom 1911). A surge genesis of these sediments was later supported by De Geer (1919), Cöster (1925), Punning et al. (1976), Haga (1978) and Rowan et al. (1982). However, there were different views with respect to the number of surges, as well as their ages. The three most recent of these studies all concluded that a major PGS surge took place in fairly recent times. Fossils of turf and driftwood buried within the marine diamicton, gave maximum ages of the last major surge of 930 ± 80 years (Rowan et al. 1982) and 605 ± 50 years BP (Punning et al. 1976).

Dahlgren et al. (unpubl.) investigated the glacial history in Van Mijenfjorden based on 3.5 kHz acoustic profiling and marine sediment cores. Four submarine lobe-shaped ice-contact sediment wedges were found. Each lobe is interpreted to record an advance–retreat cycle of the PGS (Fig. 1c), as seen from their geometry and prograding internal acoustic architecture represented by units 4, 5, 6 and 7 in Fig. 3a. Terrestrial moraines on the shores of inner Van Mijenfjorden were mapped from air photographs. The advance–retreat pattern was not conclusively seen from the morphology of the moraines alone, but each moraine could be correlated with a marine ice-contact wedge, allowing the terrestrial extent of the glacier advances to be determined. The oldest surge caused the PGS to advance 35 km beyond its present glacier front. An interpreted acoustic profile from middle to inner Van Mijenfjorden (Fig. 3a) as well as a model for the major surge event (Fig. 3b) are shown. The middle sill in Van Mijenfjorden, corresponding to the outer part of unit 4 (Fig. 3), was formed during this oldest surge event. This unit is assumed to have been deposited during the active (advance) phase of the major surge. By analogy to the observed glacier surges in Svalbard (cf. Dowdeswell et al. 1991), the active phase of the surge is inferred to have lasted no longer than 10 years, implying that unit 4 was deposited very rapidly.

During the maximum extent of the PGS surge, a glacier-dammed lake formed in Braganzavågen, a tidal flat on the inner northern side of Van Mijenfjorden (Fig. 1) (Högbom 1911; Rowan et al. 1982). This is inferred from findings of strandlines and laminated lacustrine silts up to 22 m above current sea level, suggesting a lake with a volume of approximately 0.8 km^3. A trunk of the PGS, Bakaninbreen (Bakanin Glacier), surged recently (1985–1990), but the surge front failed to reach the tidewater terminus (Hambrey et al. 1996).

Fig. 3. (a) Interpretation of a 3.5 kHz acoustic profile in Van Mijenfjorden and location of the investigated sediment cores. (b) Simplified model for the 1300 AD surging Paulabreen (Paula Glacier). (Figure modified from Dahlgren et al. unpubl.; printed with permission of the author.) Location of the profile is shown in Fig. 1c.

Materials and methods

We have investigated two gravity cores, UNIS 96-24/1 (15° 58.97' E, 77° 47.61' N; 77 m depth) and UNIS 96-23/1 (16° 06.01' E, 77°47.74' N; 58 m depth). In addition, we analysed the upper 20 cm of a box-core (UNIS 96-24/2) from the same location as UNIS 96-24/1.

Core UNIS-96-23/1 (hereafter referred to as 23/1) was retrieved on the distal slope 1 - 2 km from the reconstructed maximum position of the PGS surge. The core penetrates two main acoustic units, units 9 and 4 (Fig. 3). Unit 4 was formed during the advance phase of the major surge and unit 9 was deposited after the surge, when redeposition by gravity flows no longer occurred and the sediment wedge had stabilized. Core 24/1 is located ca. 3.5 km distally to the ice front position during the major surge, and ca.1 km distal to the toe of the abruptly terminating unit 4. It penetrates acoustic units 9 and 3. Based on the acoustic interpretations (Fig. 3), unit 3 is assumed to have been deposited prior to and during the initial phase of the major surge.

The lithology of the cores (Figs. 4, 5) was based on inspection of the split core, examination of X-ray radiographs and grain size analysis. Grain size analysis of the fraction 63 - 65 µm was performed on a Micrometrics Sedigraph 5100; fraction > 63 µm was dry sieved. Magnetic susceptibility was measured at 1 cm intervals using a Bartinton MS2E. Shear strength was measured using the fall cone test (Hansbo 1957). Total carbon (TC) was measured using a LECO IR 212. Mineral grains in the 0.5 - 1 mm and > 1 mm fractions, defined as ice-rafted debris (IRD), were counted using a binocular microscope. Preparation of the foraminiferal samples mainly followed the methods of Feyling-Hanssen (1958) and Meldgaard & Knudsen (1979). About 100 - 300 individuals of benthic foraminifera were identified from the > 100 µm fraction using a binocular

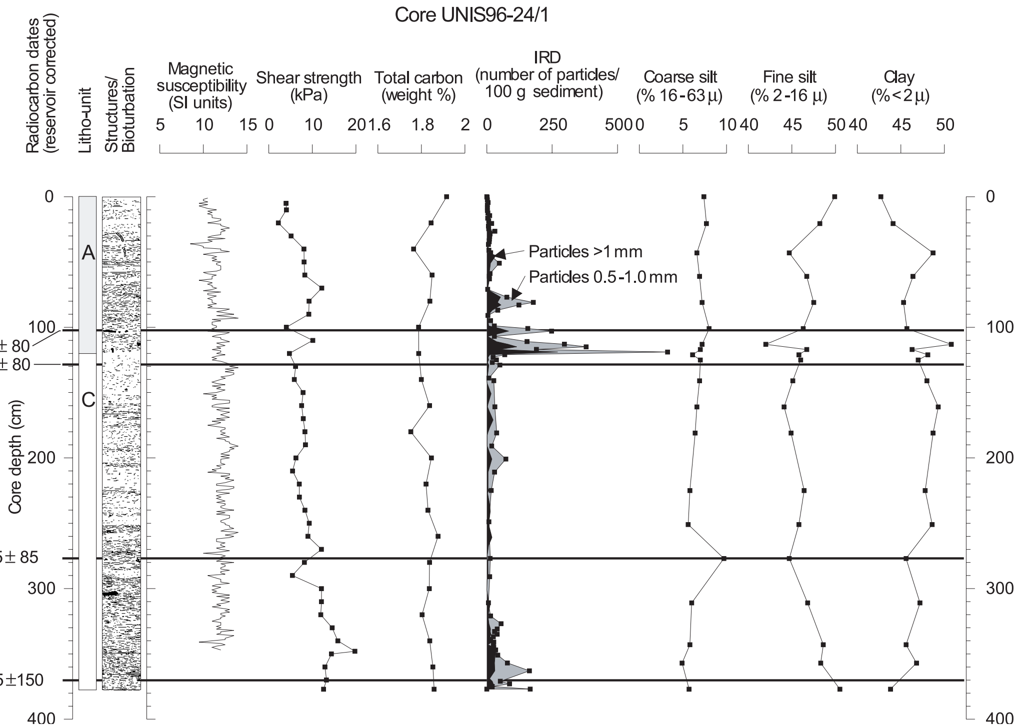

Fig. 4. Lithology in core 24/1. Radiocarbon ages are shown to the left. See legend with Fig. 5.

microscope. δ ^{18}O and δ ^{13} C measurements were performed on the benthic foraminifer *Cassidulina reniforme* at the Norwegian GMS laboratory at the University of Bergen using a Finnigan MAT 251 mass spectrometer. The reproducibility at this laboratory is 0.07 ‰ for δ ^{18}O and 0.06 ‰ for δ ^{13}C. The samples were prepared following the procedures described by Shackleton & Opdyke (1973), Shackleton et al. (1983) and Duplessy (1978). Only uncorrected isotope values are plotted (Figs. 6, 7).

Accelerator mass spectrometry (AMS) radiocarbon dates were performed on bivalve tests (Table 1, Figs. 4, 5). The targets were prepared at the Radiocarbon Laboratory in Trondheim, Norway, and were measured at the Svedberg Laboratory in Uppsala, Sweden (Table 1). All dates were corrected for a reservoir effect equal to 440 years (Mangerud & Gulliksen 1975) and calibrated to calendar year according to Stuiver et al. (1998). Age vs. core depth was estimated by linear interpolation between the dated levels and the data are plotted on a calendar year scale (Figs. 6, 7).

The upper parts of cores 24/1 and 24/2 were dated and correlated by means of ^{210}Pb and ^{137}Cs (details in Dahlgren et al. unpubl.). Dating was performed at the Risø National Laboratory, Denmark, using low background gamma counting (Appleby et al. 1986). The ^{210}Pb chronology is based on the CRS model (Appleby & Oldfield 1978) and is independently supported by the 137Cs spectra. These data were used to estimate the sediment accumulation rate in the upper part of core 24/1 (Fig. 6).

Results

Core 24/1

Two informal lithological units were identified (Fig 6). Unit A comprises the upper 120 cm of the core and is a homogeneous mud with scattered IRD. There is a sharp IRD maximum close to the A/C boundary. This IRD maximum is interpreted to reflect the major surge in Van Mijenfjorden. Two ^{14}C dates, one above and one below the

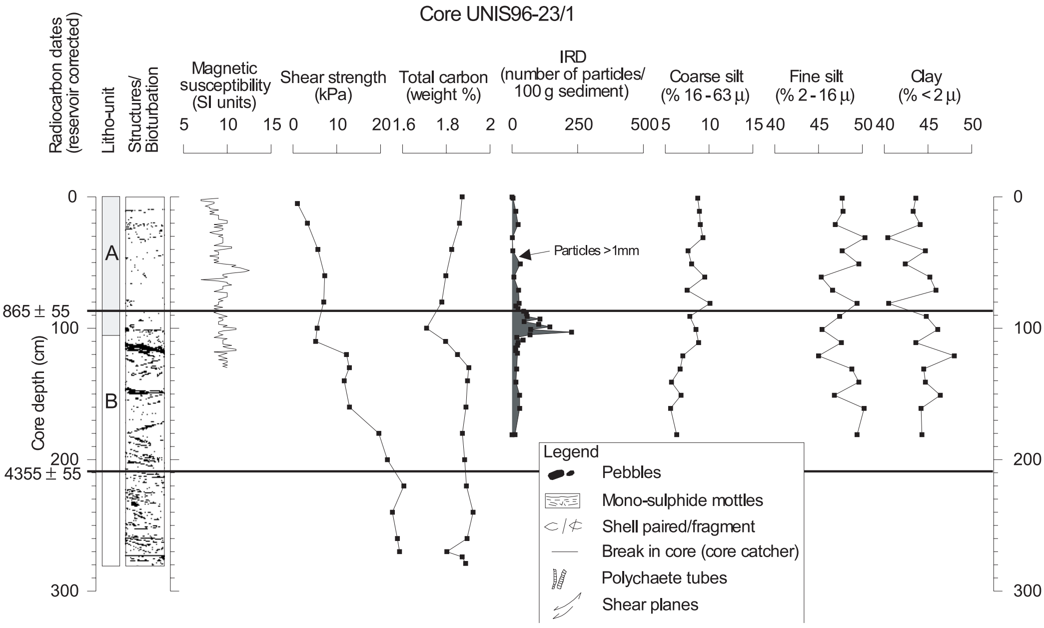

Fig. 5. Lithology in core 23/1. Radiocarbon ages are shown to the left.

IRD layer, bracket the age of the surge between 555 ± 80 and 825 ± 80 radiocarbon years BP, implying a date of ca. 1300 AD for this event. IRD generally decrease upwards in the unit except for two secondary maxima around 1480 AD and 1580 AD, respectively. Unit A corresponds to acoustic unit 9 (Fig. 3). Unit C is a homogeneous mud, distinguished from overlying unit A by its relative lack of IRD. There is a gradual rise in average rate of sediment accumulation (SAR) upwards in the core. The uppermost SAR interval, based on interpolation between the ^{14}C date 555 ± 80 and the core top (taken as 1996 AD), corresponds approximately to an average SAR based on the ^{210}Pb measurements (Fig. 6).

The foraminiferal fauna is totally dominated by the calcareous benthic species *Cassidulina reniforme* and *Elphidium excavatum*. Important accessory species are *Elphidium bartletti* and *Nonion labradoricum*. Percentage frequencies of the species are estimated based on calcareous species representing 100 %. A total of 36 benthic

Table 1. AMS (accelerator mass spectrometry) ^{14}C and calendar year age estimates from the cores used in this study. The ^{14}C dates are corrected for a reservoir effect of 440 years (Mangerud & Gulliksen 1975). The radiocarbon ages were converted to calendar years following the calibration model of Stuiver et al (1998). The radiocarbon dates are reported with ± 1σ standard deviation. A = maximum calibrated age, B= calibrated age used in age model, C= minimum calibrated age.

Core	Core depth (cm)	Lab no.	Fossil dated	^{14}C age ± 1σ	Calibrated ^{14}C age BP		
					A)	B)	C)
U96-24/1	100-104	TUa-1753	*Yoldiella frigida, Yoldiella* sp., *Darcrydium* sp.	555 ± 80	603	521	477
U96-24/1	128-130	TUa-1753	Indet. bivalve	825 ± 80	823	725	658
U96-24/1	276-278	TUa-1754	*Yoldiella nana, Musculus* sp.	1855 ± 85	1920	1822	1710
U96-24/1	368-372	TUa-1755	*Yoldiella solidula, Gastropoda* sp.	3775 ± 150	4410	4214	3979
U96-23/1	86-88	Ua-12032	*Macoma torelli*, both bivalves present	865 ± 55	859	764	702
U96-23/1	208-209	Ua-12033	*Leionucula bellotii (Nucula tenuis)*, both bivalves present	4355 ± 55	5034	4952	4853

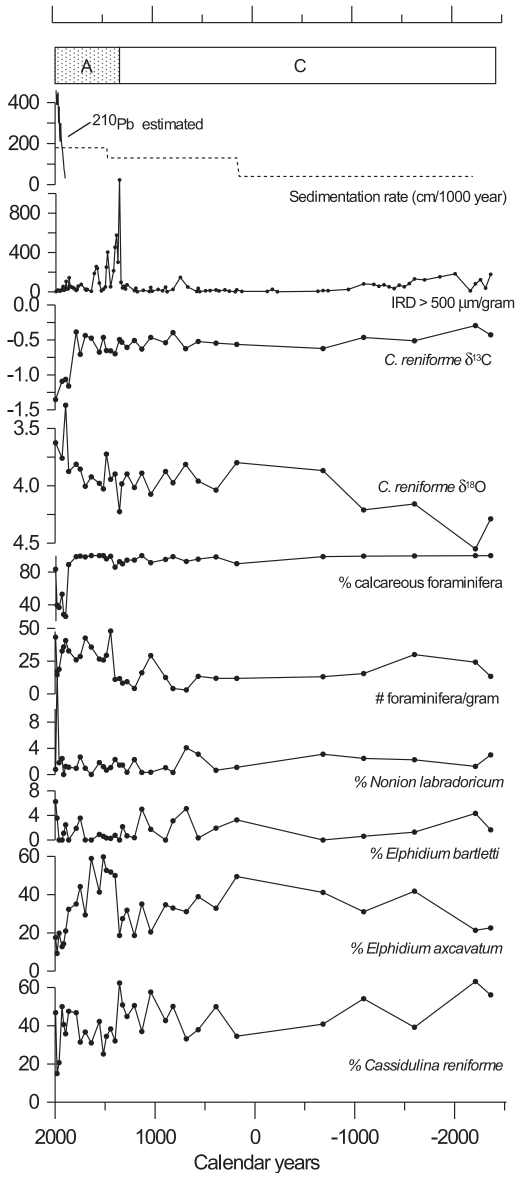

Fig. 6. Variations vs. calendar years in benthic foraminifera, foraminifera per gram sediment, % calcareous foraminifera, δ ^{18}O and δ ^{13}C, IRD and sedimentation rates in core 24/1. Lithological units are shown in the upper panel.

species have been identified in the core. Calcareous species dominate throughout the core, except in the uppermost 30 cm, which shows a marked rise in agglutinating foraminifera. These were all subsampled from the core approximately one year after the core was opened. The other samples were taken and prepared immediately after the core was opened. The reduction in carbonate of the sub-samples obtained later, is probably due to carbonate dissolution during storage of the core. Oxidation of organic matter during slow drying of the sediments, releases carbonic acid that may lower the pore water pH and cause dissolution of carbonate. We omitted from the database those samples that were extensively influenced by dissolution.

Between 400 AD to ca. 1300 AD, corresponding to upper part of unit C to the A/C boundary, *E. excavatum* showed a decline and *C. reniforme* a rise (Fig. 6). A marked minimum in foraminifera per gram straddling the A/C boundary partly predates and partly corresponds to the IRD maximum at 1300 AD. This foraminifera low was first followed by a marked rise in *E. excavatum* and decline in *C. reniforme* and then by a marked rise in foraminifera per gram. *E. bartletti* and *N. labradoricum* show a marked rise in the uppermost sample of the core. *E. excavatum* had a steady decline from ca. 1700 AD to the present.

There was a gradual decline in benthic δ ^{18}O in the lowermost part of the core, up to ca. 800 BC. This was first followed by a fairly stable interval until ca. 1750 AD, and subsequently by a ca. 0.4 ‰ decline in δ ^{18}O (Fig. 6). There was a slight depletion in δ ^{18}O corresponding to the IRD maximum at 1300 AD. There was also a δ ^{13}C depletion in the uppermost part of the core from ca. 1820 years to the present.

Core 23/1

Two lithological units are identified (Fig. 7). Unit A comprises the upper 110 cm of the core and is homogeneous mud with scattered IRD. It correlates to acoustic unit 9 (Fig. 3). IRD has a maximum close to the A/B boundary and declines upward in the unit. Unit B has less IRD and shows abundant shear structures and small scale normal faults. This unit correlates to the upper part of acoustic unit 4, which was interpreted to consist of reworked sediments, having been deposited during the advance phase of the major surge (Dahlgren et al. unpubl.). The onset of the IRD spike in the core (Fig. 5) is correlated to the onset of the IRD spike in core 24/1 (Fig. 4), dated to 1300 AD. The radiocarbon date 865 ± 40 years at 86 - 88 cm in core 23/1 overlaps with this age, when considering one sigma standard deviation of this date (Table 1).

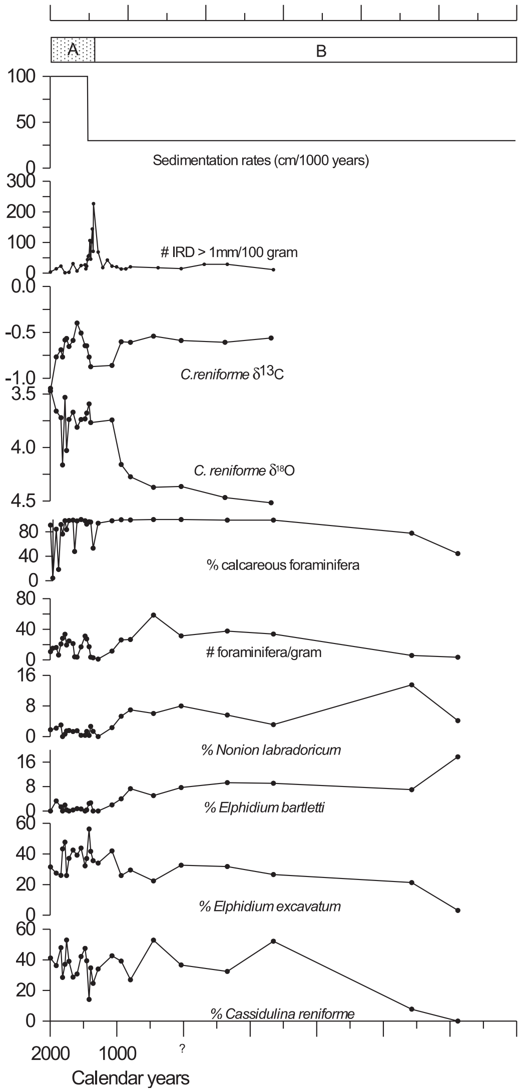

Fig. 7. Variations vs. calendar years in benthic foraminifera, foraminifera per gram sediment, % calcareous foraminifera, δ ^{18}O and δ ^{13}C, IRD and sedimentation rates in core 23/1. Lithological units are shown in the upper panel.

The core is dominated by the same species as recorded in core 24/1. A total of 36 benthic species have been identified in the core. In the upper part of unit A there are three foraminiferal subsamples showing a low calcareous foraminiferal abundance that were omitted from the database.

There is a gradual faunal shift associated with the A/B boundary (Fig. 7). Foraminiferal abundance reached a minimum around this boundary that correlates to the IRD maximum (Fig. 5). *E. excavatum* increased and had abundance spikes around 1000 AD and 1750 AD. The other species in Fig. 7 declined. *C. reniforme* appears to be inversely related to *E. excavatum*. There is a marked depletion in benthic δ ^{18}O and δ ^{13}C at the A/B boundary. δ ^{13}C reached a maximum around 1500 AD followed by a depletion up to the present (1996). Low foraminiferal abundances during the IRD maximum unfortunately prevented us from getting stable isotope measurements from this interval.

Discussion

Pre-surge palaeoceanography

As unit B correlates to the surge deposit, we consider the fossils in this unit to be glacially reworked from marine sediments deposited in inner Van Mijenfjorden prior to the surge. The elevated values of *C. reniforme* and *N. labradoricum*, relative to unit A, suggest this fauna to be reworked from an ice-front distal environment. At present these species dominate the middle and outer parts of the Svalbard fiords (Hald & Korsun 1997). An ice front distal environment is further supported by relatively high δ ^{18}O and δ ^{13}C reflecting ventilated bottom water with relatively high salinity. Higher δ ^{18}O could either be a function of lower ocean temperatures or higher salinities (less depleted by isotopically low freshwater). The higher δ ^{18}O recorded in unit B compared to A, was an effect of higher salinity rather than colder temperatures. We assume it reflects that the reworked fossils in unit B originally lived in bottom water with higher salinity, compared to the bottom water that existed during unit A. Modern bottom water temperatures in Van Mijenfjorden today are close to -1 to -1.5 OC and correspond to a core top δ ^{18}O value of ca. 3.5 ‰ (Figs 6, 7). Therefore, a δ ^{18}O enrichment relative to the modern value can only reflect a salinity increase, as further cooling is not realistic. Comparable enriched δ ^{18}O and, hence, high salinities were recorded around 2200 BC in core 24/1 associated with a fauna dominated by C. reniforme. This was followed by a gradual salinity decline until ca. 500 BC.

There are two major factors that may cause salinity variations in Van Mijenfjorden during the mid- and late Holocene: 1) influx of marine water from the open ocean as a function of sill depth changes; and 2) supply of freshwater.

Re sill depth—Due to the very shallow sill (maximum depth of 30 m) in outer Van Mijenfjorden, the exchange of water masses between the fiord and the Greenland Sea is restricted, and the inflow of oceanic, saline water is low (Skardhamar 1998). Reconstructions of sea level changes in the outer Van Mijenfjord area (Landvik et al. 1987) indicate that the sea level around 2200 BC was between 5 and 10 m above today's, due partly to a regional eustatic sea level rise and partly to glacio-isostatic depression. This would have increased the sill depth at the mouth of Van Mijenfjorden by 25 - 50 % compared with the present. It therefore seems likely that at around 2200 BC Van Mijenfjorden would have experienced a larger exchange of marine waters from the open ocean, which may also have contributed to the elevated bottom water salinities observed in our data. As the isostatic rise continued toward the present time (Landvik et al. 1987), the outer sill in Van Mijenfjorden gradually became shallower. This may explain the gradual build up of bottom freshwater in the fiord between 2200 and 500 BC indicated by the decline in benthic $\delta^{18}O$ (Fig. 6).

Re freshwater input—At present, freshwater input to Van Mijenfjorden is derived as river water originating as melting snow during summer and glacial meltwater, together with small icebergs, and is mainly a function of the precipitation in the area. Variation in precipitation during the Holocene is not well known. However, palaeoclimatic reconstructions of the Holocene in Svalbard may elucidate this question. Based on a plant macro-fossils stratigraphic study, Birks (1991) give evidence of a 1.5 - 2 °C warmer early and mid-Holocene, followed by cooling the last 4000 years. This temperature history is supported by Salvigsen et al. (1992) showing increased abundance of the thermophilic molluscs during early and mid-Holocene. Further, Svendsen & Mangerud (1997) have shown a glaciation minimum between early Holocene (Preboreal) and 3000 ^{14}C years BP. They also show that glaciers in Svalbard started to advance 4000 - 5000 ^{14}C years ago with some reaching the ocean 2000 - 3000 years ago. A similar glacial history is reconstructed further to the east in Franz Josef Land (Lubinski et al. 1999). The glacial history in Svalbard and Franz Josef Land appears to mainly reflect the Holocene temperature history and variations in influx of Atlantic Water to the European Arctic (Svendsen & Mangerud 1997; Lubinski et al. 1999). These investigations are in accordance with the atmospheric temperature history extracted from the Greenland ice cores (cf. Johnsen et al. 1992), indicating an early to mid-Holocene climate optimum followed by a cooling in the late Holocene. At present there is a close correlation between atmospheric temperature and precipitation in the North Atlantic region. Assuming that was also the case for the Holocene, it would support increased precipitation during the warm early and mid-Holocene and reduced precipitation during the colder late Holocene. Therefore, the reduction in the salinity of Van Mijenfjord should correspond to a period where reduced precipitation seems likely. From this we conclude that the freshwater increase in Van Mijenfjorden between 2200 BC to 500 BC was not forced by increased freshwater precipitation, but rather was driven mainly by reduced saltwater inflow to the fiord due to a shallowing of the outer sill.

Palaeoceanography during and after the surges

The large IRD spike observed around 1300 AD in both the investigated cores (Figs. 5, 6) is interpreted to reflect the major surge in Van Mijenfjorden (Dahlgren et al. unpubl.). The age of this event compares well to minimum and maximum ages obtained by dating the till deposits on land (Punning et al. 1976; Rowan et al. 1982). During this event the PGS ice front advanced to a position 35 km beyond its present front, and acoustic unit 4 was deposited very rapidly. The minimum in foraminifera per gram associated with this IRD spike indicates that production was suppressed during this event or that the foraminiferal abundance was masked by high sediment input. However, immediately after the major IRD spike, production increased and/or masking slowed down rapidly, as indicated by the marked rise in foraminiferal abundance (Fig. 6). Faunal change was mainly due to a large increase in *E. excavatum*, a species known to dominate in turbid water masses close to glacier termini in fjords of both Svalbard (Hald & Korsun 1997) and Novaya Semlja (Korsun & Hald 1998). Hence, the faunal changes imply that near-glacial environments, reflected by high abundances of *E. excavatum,* prevailed for approximately 300 years until a marked decline in *E. excavatum* occurred, starting between 1700 AD and 1640 AD in core 24/1 (Fig. 6) and somewhat later in core 23/1 (Fig. 7).

The rise in *E. excavatum* just after the major IRD event, is associated with a slight $\delta^{18}O$ depletion. This may indicate that bottom water salinities were slightly reduced during this phase of the surge. However, the decline in $\delta^{18}O$ following the major IRD spike suggests a gradual decrease in bottom water salinities in the Van Mijenfjorden during the last ca. 600 years. This decrease is also associated by a marked $\delta^{13}C$ depletion.

We assume there has been little change in the water exchange between the fiord and the open ocean during the last 600 years linked to post glacial uplift as the isostatic rise slowed down (Landvik et al. 1987). Therefore, the cause of the salinity decrease should reflect either increased supply of fresh meltwater to the fiord, or other changes in the regional oceanography of the polar North Atlantic.

The glacial history of Van Mijenfjorden may support the idea of increased meltwater input. Dahlgren et al. (unpubl.) have shown that the Paulabreen system advanced at least three times following the major 1300 AD surge (Fig. 1c). Though these events are not well dated, some age limitations can be made. Their surge-associated deposits are all situated inside the 1300 AD surge deposit (Fig. 1); therefore, these surges must be younger than 1300 AD. The glacier advance associated with the innermost and youngest surge, is only some 200 m outside the 1898 ice front. During the series of surges the ice volume of the PGS has become significantly smaller. In addition, the PGS has retreated less than 10 km since 1898. We infer that the PGS may have lost an equivalent of 30 - 40 % of its present total ice volume during the series of surges between 1300 AD and > 1898 AD and subsequent retreat the last century. This volume is estimated at 12 - 16 km^3. This would have produced meltwater of ca. 0.05 Sv (1 Sv = $10^6 m^3 s^{-1}$), averaged over the 700 year period from 1300 AD to the present. The timing of this loss of ice volume compares well to the salinity depletion. We therefore suggest that increased supply of glacial meltwater/icebergs contributed to the salinity depletion during the last ca. 700 years.

In addition, oceanographic changes outside Van Mijenfjorden may also have contributed to the changes. There is evidence, for example, of changing ocean temperatures in the Norwegian and Arctic seas during the last millennium (Overpeck et al. 1997), including the Medieval Warm Period (prior to 1500 AD), the Little Ice Age (after 1500 AD followed by the warming during the last 100 years). These changes may be linked to changes in the North Atlantic heat flux. However, their implications for the changes in Van Mijenfjorden are not easy to evaluate and would require comparison with a detailed millennium scale record from e.g. offshore western Svalbard. The marked $\delta^{13}C$ depletion in Van Mijenfjorden the last ca. 500 years may be linked to changes in foraminiferal sediment habitat, rather than changes in the fiord bottom water characters. The last ca. 100 years of the $\delta^{13}C$ depletion correlates to a marked rise in sedimentation rates. *C. reniforme*, the species used for the stable isotopic measurements, has an infaunal habitat and its $\delta^{13}C$ composition to a large degree reflect that of the ambient pore water. During increased sedimentation, carbonate $\delta^{13}C$ would become depleted reflecting less ventilated pore water.

Mixing of freshwater to bottom

Today, most of the freshwater issuing from the rivers and melting glaciers during summer occupies the uppermost water column due to its relatively low density. However, the reduction in salinity over the last 2000 years inferred by the present study suggests that freshwater is mixed all the way down to the fiord bottom. Such vertical mixing may take place due to different processes (Freeland et al. 1980). During summer there is a marked freshwater outflow across the outer sill in Van Mijenfjorden. Entrainment of saltier water in this outflow may cause a reduction in the salinity of the fiord (V. Tverberg, pers. comm. 1999). Wind, tidewater currents and freshwater supply contribute to a circulation pattern in Van Mijenfjorden that include mixing of the upper 10 - 20 m of the water column (Skardhamar 1998). Another important process for vertical mixing is sea ice formation. When sea ice freezes during the fall, brine—characterized by very low temperatures and high salinity—is rejected to the deeper water layer. This probably explains the very cold bottom water in Van Mijenfjorden today (Skardhamar 1998). As brine formation takes place in the surface water, it also attains a low $\delta^{18}O$ composition. The brine rapidly sinks through the water column and thereby brings $\delta^{18}O$-depleted water to the bottom as well as entrained fresher water to deeper layers. Low salinity water may also be transported to the bottom as sediment laden meltwater plumes. However, suspended sediment concentration greater than 30 kg m^{-3} is needed to overcome the density contrasts between the ice tunnel fluid (turbid but freshwater) and normal sea water, and thus cause the issuing plume to sink (Syvitski & Shaw 1995). Sediment concentrations are seldom this high, even during flood conditions (Syvitski et al. 1987), although surges are an exception. Thus, we consider this process to be of less importance for the salinity reduction in the Van Mijenfjorden. A possible exception may be the slight $\delta^{18}O$ depletion related to the major 1300 AD surge.

Conclusions

Cores 23/1 and 24/1 record changes in the palaeoceanography of Van Mijenfjorden throughout the last ca. 4000 years. Stable isotope measurements of benthic foraminiferal $\delta^{18}O$ and $\delta^{13}C$ suggest well ventilated bottom water around 2200 BC that was saltier than today. This period correlates in time to a period of greater oceanic exchange between the fiord and open ocean than today. These conditions were probably forced by a deeper threshold in the outer fiord due to the high relative sea level. A gradual decline in bottom water salinity took place between 2200 BC and 500 BC. During this period communication to the open ocean decreased as a function of glacio-isostatic rebound, establishing the sill depth in the outer fiord close to the modern value of –25 m.

A major surge event occurred around 1300 AD during which the tidewater Paulabreen system (PGS) advanced 35 km beyond its present limit. This event is recorded as a marked IRD peak in the sediment cores and is followed by a number of surges—minimally three—up to the present time (Fig. 3). Benthic foraminifera reflect the major surge with a change towards an assemblage typical of near-glacier environments of Arctic fiords. As the ice margin retreated during the subsequent surges, the foraminiferal fauna was replaced by a more glacier-distal assemblage. There was a 0.5 ‰ decline in bottom water $\delta^{18}O$ from the first major surge to the present. This is interpreted as mainly reflecting increased glacial meltwater flux to the fiord. During the surges and subsequent retreat the last century, the PGS lost as much as 30 – 40 % of its total volume. This represent a meltwater flux corresponding to 0.05 Sv that may explain the freshwater build-up in the fiord during the last 700 years. This study indicates that surging glaciers may have a large effect on the climate and oceanography in a fiord system. This observation may possibly have wider relevance regarding ice sheet behaviour during the Late Quaternary.

Acknowledgements.—The sediment cores and acoustic profiles were collected during cruises in 1996 and 1997 on the *R/V Jan Mayen*. Helmar Kunzendorf performed the ^{210}Pb and ^{137}Cs measurements. The AMS ^{14}C dates were supervised by Steinar Gulliksen (Trondheim) and Göran Possnert (Uppsala) and the stable isotope analysis by Eystein Jansen (Bergen). Assistance at the University of Tromsø was provided by Elsebeth Thomsen (bivalve identification), Marit Berntsen and Mary Raste (laboratory analysis), Gunvor Granaas (photography), Audun Igesund and Jan P. Holm (computer drawing), Steinar Iversen (acoustic profiling) and Annbjørg Johansen (administration). Funding was provided to MH from the Norwegian Research Council to the Strategic University Programme Sedimentary Processes and Paleoenvironment in Northern Fjords (SPINOF) and to EL from the University Courses on Svalbard (UNIS). This manuscript benefited from discussions with Anne Jennings and James Syvitski. Jon Landvik and one anonymous person reviewed the paper. To all these persons and institutions we extend our sincere thanks.

References

Appleby, P. G., Nolan, P. J., Gifford, D. W., Godfrey, M. J., Oldfield, F., Anderson, N. J. & Battarbee, R. W. 1986: 210-Pb dating by low background gamma counting, *Hydrobiologica 143*, 21–27.

Appleby, P. G. & Oldfield, F. 1978: The calculation of lead-210 dates assuming a constant rate of supply of unsupported 210-Pb to the sediment. *Catena 5*, 1–8.

Birks, H. H. 1991: Holocene vegetational history and climate change in west Spitsbergen—plant macrofossils from Skardtjørna, an Arctic lake. *The Holocene, 1*, 209-218.

Cöster, F. 1925: Quaternary geology of the region around the Kjellstrøm Valley. *Geogr. Ann. VII*, 104–121.

Dahlgren, T., Lebesbye, E., Hald, M. & Kunzendorf, H. Unpubl. ms. Sediment release from high Arctic glaciers as recorded in late Holocene fjord sediment, Van Mijenfjorden, Spitsbergen.

De Geer, G. 1919: Spetsbergens natur i Sveagruvans omnejd. (Spitsbergen's nature in the Svea mine area.) *Ymer 4*, 240–277.

Dowdeswell, J. & Dowdeswell, E.-K. 1989: Debris in icebergs and rates of glaci-marine sedimentation; observations from Spitsbergen and a simple model. *J. Geol. 92*, 221–231.

Dowdeswell, J., Hamilton, G. S. & Hagen, J. O. 1991: The duration of the active phase on surge-type glaciers: contrasts between Svalbard and other regions. *J. Glaciol. 37*, 388–400.

Duplessy, J.-C. 1978: Isotope studies. In J. R. Gribbin (ed.): *Climatic change*. Pp. 46–67. Cambridge: Cambridge University Press.

Feyling-Hanssen, R. W. 1958: Mikropaleontologiens teknikk. (Micropalaeontological techiniques.) *Norwegian Geotechnical Institute 29*, 1–14.

Freeland, H., J., Farmer, D. M. & Levings, C. D. 1980: *Fjord oceanography.* New York: Plenum Press.

Gulliksen, B., Holte, B. & Jakola, K.-J. 1985: The soft bottom fauna in Van Mijenfjord and Raudfjord, Svalbard. In J. S. Gray & M. E. Christiansen (eds.): *Marine biology of polar regions and effects of stress on marine organisms.* Pp. 199–215. New York: John Wiley & Sons.

Haga, Ø. 1978: *Morenemasser i dødis etter et brefremstøt i Van Mijenfjorden. (Till deposits in dead ice from a glacier advance in Van Mijenfjorden.)* Thesis, University of Oslo.

Hagen, J. O., Roland, E. & Jørgensen, T. 1993: *Glacier atlas of Svalbard and Jan Mayen. Nor. Polarinst. Medd. 129.* Oslo: Norwegian Polar Institute.

Hald, M. & Korsun, S. 1997: Distribution of modern Arctic benthic foraminifera from fjords of Svalbard. *J. Foraminifer. Res. 27*, 101–122.

Hambrey, M. J., Dowdeswell, J., Murray, T. & Porter, P. R. 1996: Thrusting and debris entrainment in a surging glacier: Bakaninbreen, Svalbard. *Ann. Glaciol. 22*, 241–248.

Hansbo, S. 1957: *A new approach to determination of shear strength of clay by the fall cone test. Royal Swedish Geotechnical Institute Proceedings 14.*

Harland, W. B. 1997: *The geology of Svalbard. Geol. Soc. Mem. 17.* London: Geological Society.

Högbom, B. 1911: Bidrag till Isfjordområdets kvarærgeologi. (On the Quaternary geology of the Isfjorden area.) *Geol. Fören. Stockholm Förh. 33*, 32–57.

Hopkins, T. S. 1991: The GIN Sea—a synthesis of its physical oceanography and literature review 1972–1985. *Earth Sci. Rev. 30*, 175–318.

Jiskoot, H., Murray, T. & Boyle, P. 2000: Controls on the distribution of surge-type glaciers in Svalbard. *J. Glaciol. 46*, 412–422.

Johnsen, S. J., Clausen, H. B., Dansgaard, W., Gundestrup, N. S., Hansson, M., Jonsson, P., Steffensen, J. P. & Sveinbjørndottir, A. E. 1992: A "deep" ice core from east Greenland. *Medd. Grønl. Geosci. 29*, 3–22.

Korsun, S. & Hald, M. 1998: Modern benthic foraminifera off tide water glaciers, Novaja Semlja, Russian Arctic. *Arct. Alp. Res. 30*, 61–77.

Landvik, J. Y., Mangerud, J. & Salvigsen, O. 1987: The late Weichselian and Holocene shoreline displacement on the west–central coast of Svalbard. *Polar Res. 5*, 29–44.

Lubinski, D. L., Forman, S. L. & Miller, G. H. 1999: Holocene glacier and climatic fluctuations on Franz Josef Land, Arctic Russia, 80° N. *Quat. Sci. Rev. 18*, 85–108.

Mangerud, J. & Gulliksen, S. 1975: Apparent radiocarbon ages of recent marine shells from Norway, Spitsbergen, and Arctic Canada. *Quat. Res. 5*, 263–273.

Meldgaard, S. & Knudsen, K. L. 1979: Metoder til indsamling og oparbejdning af prøver til foraminifer-analyser. (Methods for sampling and processing of samples for foramineral analysis.) *Dansk Natur Dansk Skole Årsskrift 1979, 48–57.*

Mosby, H. 1968: In A. Sømme (ed.): *Geography of Norden.* Pp. 18–26, map 7. Oslo: J. W. Cappelen.

Murray, T., Dowdeswell, H. A., Drewry, D. J. & Frearson, I. 1998: Geometric evolution and ice dynamics during a surge of Bakaninbreen, Svalbard. *J. Glaciol. 44*, 263–272.

Overpeck, J., Hughen, K., Hardy, D., Bradley, R., Case, R., Douglas, M., Finney, B., Gajewski, K., Jacoby, G., Jennings, A., Lamoureux, S., MacDonald, G., Moore, J., Retelle, M., Smith, S., Wolfe, A. & Zielinski, G. 1997: Arctic environmental changes of the last four centuries. *Science 287*, 1251–1256.

Punning, J.-M., Troitsky, L. & Rajamae, R. 1976: The genesis and age of the Quaternary deposits in the eastern part of Van Mijenfjorden, West Spitsbergen. *Geol. Fören. Förh. 98*, 343–347.

Rowan, D. E., Pewe, T. L. & Pewe, R. H., 1982: Holocene glacial geology of the Svea lowland, Spitsbergen, Svalbard. *Geogr. Ann. 64A*, 35–51.

Salvigsen, O., Forman, S. L. & Miller, G. H. 1992: Thermophilous molluscs on Svalbard during the Holocene and their paleoclimatic implications. *Polar Res. 11*, 1–10.

Salvigsen, O. & Winsnes, T. O. 1989: *Geological map of Svalbard 1:100,000. Sheet C10G Braganzavågen map. Nor. Polarinst. Temakart 4.* Oslo: Norwegian Polar Institute.

Shackleton, N. J., Imbrie, J. & Hall, M. A. 1983: Oxygen and carbon isotope record of The east Pacific core V19-30: implications for the formation of deep water in the late Pleistocene North Atlantic *Earth Planet. Sci. Lett. 65*, 233–244.

Shackleton, N. J. & Opdyke, N. D. 1973: Oxygen isotope and palaeomagnetic stratigraphy of equatorial Pacific core V28-238: oxygen isotope temperatures and ice volume on a 10^5 year and 10^6 year scale. *Quat. Res. 3*, 39–55.

Skardhamar, J. 1998: *Sirkulasjonen i Van Mijenfjorden, en arktisk fjord. (Circulation in Van Mijenfjorden, an Arctic fiord.)* Thesis, Dept. of Geophysics, University of Bergen.

Steel, R. J. & Worsley, D. 1984: In A. M. Spencer et al. (eds.) *Petroleum geology of the northern European margin*. Pp. 109–135. London: Graham and Trotman.

Stuiver, M., Reimer, P., J., Bard, E., Beck, J., W., Burr, G. S., Hughen, K. A., Kromer, B., McCormac, G., van der Plicht, J. & Spurk, M. 1998: INTCAL98 Radiocarbon age calibration, 24,000-0 cal BP. *Radiocarbon 40*, 1041–1083.

Svendsen, J. I. & Mangerud, J. 1997: Holocene glacial and climatic variations on Spitsbergen, Svalbard. *The Holocene 7*, 45–57.

Syvitski, J. P. M., Burrell, D. C. & Skei, J. M. 1987: *Fjords: processes and products.* New York: Springer.

Syvitski, J. P. M. & Shaw, J. 1995: In G. M. P. Perillo (ed.): *Geomorphology and sedimentology of estuaries. Dev. Sedimentol. 53*, 113–178.

Vinje, T. 1985: The physical environment, the western Barents Sea. Drift, composition, morphology and distribution of the sea ice fields in the Barents Sea. *Nor. Polarinst. Skr. 179c*, 26. Oslo: Norwegian Polar Institute.

Wadhams, P. 1981: The ice cover in the Greenland and Norwegian seas, *Rev. Geophys. Space Phys. 19*, 345–393.